Materials Science and Engineering A 502 (2009) 54–63

Contents lists available at ScienceDirect

Materials Science and Engineering A

journal homepage: www.elsevier.com/locate/msea

Analysis of ductile cast iron tensile tests to relate ductility variation to casting defects and material microstructure

Karl-Fredrik Nilsson*, Vratko Vokál

European Commission, DG-JRC, Institute for Energy, 1755 ZG, Petten, The Netherlands

ARTICLE INFO

Article history:
Received 26 June 2008
Received in revised form
24 September 2008
Accepted 26 September 2008

Keywords:
Ductile cast iron
Ductility
Casting defects
Probabilistic fracture mechanics
Tensile tests

ABSTRACT

This paper describes an experimental and analytical study to correlate the ductility variation in ductile cast iron to casting defects and the cast iron's microstructure. A large set of specimens from three manufactured components were tested to derive statistical distributions of tensile and fracture properties. Eighty-one of 150 tested tensile specimens were analyzed by metallography and fractography to identify and size defects and microstructural variations. It was found that the elongation at fracture was reduced by casting defects in the form of magnesium-oxide films and to a lesser extent by the graphite properties and pearlite content. The paper presents an elastic–plastic probabilistic fracture mechanics model that relates the variation in ductility to the size and shape of casting defects. The agreement between computed and measured results is quite good.

1. Introduction

The microstructure of ductile cast iron depends on the spheroidizing of graphite, the alloying elements, the casting temperature and possible post heat treatment. The material properties, in particular the ductility, may vary significantly due to casting defects and variations in microstructure. The graphite morphology plays an important role and the more the graphite shape deviates from the ideal spherical shape the lower is the ductility and strength [1–4]. Ductile cast iron may also have a number of volumetric defects (pores, blow holes), inclusions and planar defects from oxide and carbon films [1,2]. The matrix material plays also an important role where the softer ferrite gives higher ductility but lower yield strength than pearlite. Empirical relations between material properties such as elongation or tensile strength and microstructural properties are often used in design. There have also been relatively successful attempts to relate elongation to the relative area of defects and loss of load bearing area [5,6] or by using fracture mechanics [7].

This paper deals specifically with how the ductility variation in three different ductile cast iron inserts for radioactive waste disposal depends on the magnesium-oxide film defects and graphite properties. The paper goes beyond the earlier investigation of this material, e.g. [8,9], by adopting a more advanced microstructural characterization technique and by including crack growth resistance effects in the probabilistic fracture model. The computed distribution of elongation at fracture is not sensitive to crack growth resistance effects but crack growth resistance effects need to be included for accurate sizing of the defects. The outline of the paper is as follows. The statistical test plan and the results of the mechanical tests are presented first. This is followed by a description of the microstructural analysis of tested specimen to relate defects and microstructure to ductility. The probabilistic fracture mechanics model is then presented to correlate the size and shape of casting defects to the variation in ductility.

2. Experimental work

2.1. Statistical test plan

Three different inserts referred to as I24, I25 and I26 were used for the material characterization tests. The chemical compositions of the non-FE elements are given in Table 1. The inserts have a length of about 5 m and a diameter of 1 m. Each insert contains 12 channels with dimension 180 mm × 180 mm and length slightly shorter than the total insert length [8,9]. The wall thickness between the channels is approximately 50 mm. For each insert a slab from the solid bottom and a slab from the top, which contains fuel channels, were cut out and used for specimen preparation. Specimens were taken at different locations and with different orientations of top and bottom. Tensile, compression and fracture tests were performed on a large set of specimens, in accordance

* Corresponding author. Tel.: +31 224 565420; fax: +31 224 565641.
E-mail address: karl-fredrik.nilsson@jrc.nl (K.-F. Nilsson).

0921-5093/$ – see front matter © 2008 Elsevier B.V. All rights reserved.
doi:10.1016/j.msea.2008.09.082

Table 1
Chemical analysis (weight percentage) of non-Fe elements in ductile iron canister inserts I24, I25 and I26.

Canister insert	C (%)	Si (%)	Mn (%)	P (%)	S (%)	Cr (%)	Ni (%)	Mo (%)	Cu (%)	Mg (%)
I24	3.66	2.31	0.15	0.03	0.01	0.03	0.27	0.01	0.11	0.05
I25	3.78	2.08	0.21	0.01	0.01	0.04	0.50	–	–	0.04
I26	3.56	2.39	0.52	0.03	0.01	–	0.73	–	–	0.06

Table 2
The parameter values for the Ramberg–Osgood deformation plasticity model and the fracture toughness values for the three inserts.

Insert	Tensile parameters				Fracture toughness			
	E (GPa)	σ_0 (MPa)	α	n	Crack initiation	Crack growth resistance		
					J_{IC} (kN/m)	a_1	a_2	a_3
I24	170	182	0.53	6.23	47	−0.069	0.462	3.66
I25	170	177	0.61	6.06	58	−0.094	0.420	3.84
I26	170	203	0.26	6.67	32	−0.090	0.494	3.13

with standard test procedure [10,11]. In total there were about 150 tensile, 50 fracture and 20 compression specimens. Most tensile specimens had a diameter of 14 mm but some had 9.5 mm or 20 mm to assess statistical size effects.

2.2. Tensile and fracture tests

There was a large variation for the elongation at fracture between different specimens from the same insert but the stress–strain curves up to failure were almost identical. The stress–strain curve for insert I26 displayed more hardening than I24 and I25 due to its higher manganese content which promotes pearlite formation. The inserts I24 and I25 had very similar stress –strain curves. A Ramberg–Osgood deformation plasticity model was adopted to describe the stress–strain behaviour,

$$\varepsilon = \frac{\sigma}{E}\left[1 + \alpha\left(\frac{\sigma}{\sigma_0}\right)^{n-1}\right]. \quad (1)$$

The fitted parameters E,σ_0,α and n for the three inserts are given in Table 2. The fit with the experimental data is very good for the three inserts [9].

Fig. 1 shows the mean value and standard deviations for elongation at fracture for specimens from the three inserts taken from the bottom and two orientations in the upper part of the insert. It is apparent that there is a large variation in ductility between the three inserts as well as within inserts and that the original requirement that the elongation should be below 11% is generally not satisfied. Insert I25 had the smallest variation in elongation at fracture. For insert I26 and in particular I24, the ductility was higher for specimens from the bottom than from the top slab. The higher ductility in the bottom is related to the smaller number of magnesium-oxide films as explained below. There are two reasons for why one should expect more defects in the top. First, the fuel channels in the upper part act as heat sinks during the casting process which causes a difference in the solidification rate and thereby promotes material variability and second, the magnesium films may migrate upwards when the casting is in its liquid phase. The specimens were denoted by the insert (I24, I25 or I26), the location and orientation (BT for bottom transverse L or T for transverse or longitudinal from the top or U for top without distinction L/T) and the specimen diameter (S = 9.5 mm, M = 14 mm and L = 20 mm)

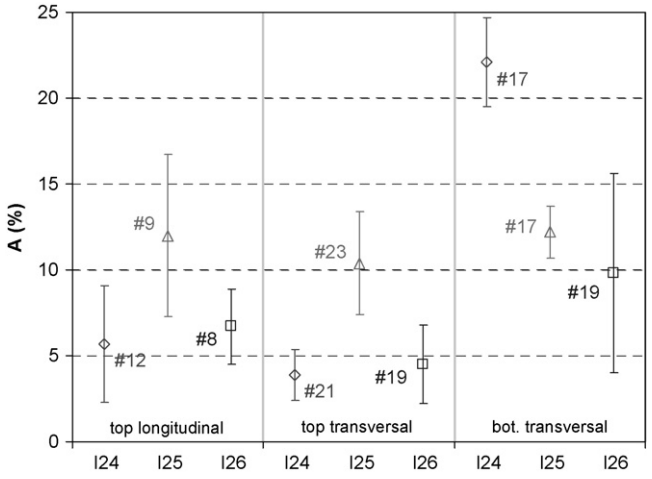

Fig. 1. Elongation after fracture: mean values and ±standard deviation plotted for (i) canister insert (I24, I25, I26), (ii) sampling region (top, bottom) and (iii) specimen orientation. (#) Indicates the number of tests per set.

The mean values for fracture toughness for crack growth initiation, J_{IC}, were 47, 58 and 32 kN/m with standard deviations 10, 9 and 5 kN/m for I24, I25 and I26, respectively. All inserts had significant crack growth resistance. The crack growth resistance curves were fitted to the formula,

$$J_R(da) = J_{IC} + e^{a_3 + a_2 \ln(da) + a_1 (\ln(da))^2}. \quad (2)$$

In Eq. (2) J is in kN/m and da in mm. The values for a_1, a_2 and a_3 are given in Table 2.

2.3. Fractographic and metallographic analysis of tensile specimens

The conjecture was that the large variation in ductility was related to material microstructure and casting defects. A microstructural analysis was therefore performed for 81 of the tested 150 tensile specimens using a 1 cm segment cut from one of the two fractured ends of the broken specimen. The investigated specimens had roughly the same distribution as the complete set with respect to ductility, insert and location (top or bottom) in order correlate the observations to the complete set of tests by statistical analyses.

The surface from the cut end of the segment was analysed by high resolution scanning electron microscope (SEM) in backscattered electrons (BEI) imaging mode and optical microscope. The image analysis of the matrix constituents and the graphite parame-